

Revisiting the Thermal Relaxations of Poly(vinyl alcohol)

J. Betzabe Gonzalez-Campos,¹ Zaira Y. Garcia-Carvajal,² E. Prokhorov,²
J. Gabriel Luna-Barcenas,² M. E. Mendoza-Duarte,³ Javier Lara-Romero,¹
Rosa E. del Rio,¹ Isaac C. Sanchez⁴

¹Universidad Michoacana de San Nicolás de Hidalgo, Ciudad Universitaria, Morelia, Michoacán 58060, México

²Cinvestav Querétaro, Libramiento norponiente No. 2000, Fracc. Real de Juriquilla, Querétaro, Qro. 76230, México

³Centro de Investigación en Materiales Avanzados, Chihuahua, Chihuahua 31109, México

⁴Department of Chemical Engineering, University of Texas at Austin, Austin, Texas 78703

Received 11 June 2010; accepted 13 October 2010

DOI 10.1002/app.33615

Published online in Wiley Online Library (wileyonlinelibrary.com).

ABSTRACT: The molecular dynamics of poly(vinyl alcohol) (PVA) were studied by dielectric spectroscopy and dynamic mechanical analysis in the 20–300°C range. The well-established plasticizing effect of water on the glass-transition temperature (T_g) of PVA was revisited. Improper water elimination analysis has led to a misinterpretation of thermal relaxations in PVA such that a depressed T_g for wet PVA films (ca. 40°C) has been assigned as a secondary β relaxation in a number of previous studies in the literature. In wet PVA samples, two different Vogel–Fulcher–Tammann behaviors separated by the moisture evaporation region (from 80 to 120°C) are observed in the low- (from 20 to 80°C) and high- (>120°C) temperature ranges. Previously, these two

regions were erroneously assigned to two Arrhenius-type relaxations. However, once the moisture was properly eliminated, a single non-Arrhenius α relaxation was clearly observed. X-ray diffraction analysis revealed that the crystalline volume fraction was almost constant up to 80°C. However, the crystallinity increased approximately 11% when temperature increased to 180°C. A secondary β_c relaxation was observed at 140°C and was related to a change in the crystalline volume fraction, as previously reported. © 2012 Wiley Periodicals, Inc. *J Appl Polym Sci* 000: 000–000, 2012

Key words: dielectric properties; glass transition; molecular dynamics

INTRODUCTION

For many years, poly(vinyl alcohol) (PVA) has been investigated extensively by a large number of techniques to gain a better understanding of its physical and chemical properties. Because of its good film-forming properties, excellent mechanical properties, biocompatibility, nontoxicity, flexibility, easy preparation, excellent chemical resistance, and its ability to be crosslinked without any chemical agent, PVA has been used in a wide variety of applications, which include the biomedical field, sensors, the food industry, and fuel cells, to name a few. This synthetic polymer has been blended and chemically modified with a high number of natural polymers and inorganic compounds to improve or enhance specific properties, for example, the conductivity¹ or mechanical properties.² On the other hand, it has been shown by differential scanning calorimetry, dynamic mechani-

cal analysis (DMA), and dielectric spectroscopy (DS) that the glass-transition temperature (T_g) of PVA can be modified by the inclusion of ions, ceramics, monomers, nanoparticles, nanotubes, and other polymers.^{3–9} In this context, an accurate T_g characterization plays a crucial role in polymer science because it indicates the change from the glassy state into a liquid or a rubbery state. T_g can be a measure of compatibility or miscibility in polymer blends.¹⁰ Additionally, the physicochemical properties, such as dissolution, bioavailability, processing, and handling qualities, of a material can be related to the material's T_g .¹¹ Also, a plasticizing effect of small amounts of water on T_g can lead to slight differences in the T_g values reported elsewhere.⁹

Because of all the aspects mentioned previously, it is necessary to fully understand the nature of the molecular motions in this polymer to obtain information about the structural properties of this material; that is, relaxations play an important role in controlling the macroscopic properties. Thereby, DS and DMA have been carried out on PVA films to study its molecular motion and structural transitions.^{1,5,6,12–20} Primary, secondary, and crystalline relaxations have been reported by DS^{6,13,21} and DMA in pristine PVA and PVA systems.^{16,17} Secondary

Correspondence to: J. G. Luna-Barcenas (gluna@qro.cinvestav.mx).

Contract grant sponsor: Consejo Nacional de Ciencia y Tecnología of México.

relaxations in PVA have been shown to be related to the rotation of OH side groups and local twisting motions about the main chain, as observed by mechanical and dielectric measurements.²² The mechanical results include additional processes, named γ modes, often observed around -70°C and associated with localized rotations of hydroxyl groups or absorbed molecules.^{9,22} Also, important effects on amorphous relaxations induced by changes in the crystalline–amorphous phases have been reported.^{22,23} Furthermore, the strong influence of the absorbed water on the polymer structure and molecular mobility is well established.²⁴

Even in the numerous dielectric studies related to PVA, dielectric measurements have been commonly carried out below 135°C ,^{1,5,12–15,18,20,21} with important aspects such as moisture and crystallinity neglected. These physical properties can lead to discrepancies in the interpretation of the relaxation processes in PVA. In the temperature range 30 – 100°C , the temperature dependence of the conductivity and the relaxation time (τ) have been commonly described as Arrhenius-type behavior. This behavior can be ascribed to a secondary relaxation process and is related to the rotation of hydroxyl groups.^{1,13,15,25–27} Nevertheless, other authors have observed VTF behavior associated with a primary relaxation process.^{5,12,18} Thermal relaxations of PVA in this temperature range have been the subject of contradictory interpretations; therefore, a deep analysis in a wider temperature range is needed to gain better insight into the molecular dynamics of PVA and its blends, composites, and PVA-based materials.

The aim of this study was to examine PVA molecular dynamics by DS and DMA in a wider temperature range to shed light into PVA molecular motions. The influence of the moisture content and change in crystalline volume fraction as a function of temperature was addressed in detail to prevent misinterpretation of the nature of the PVA molecular motions. X-ray diffraction (XRD), differential scanning calorimetry, and thermogravimetric analysis (TGA) were used to complement this study.

EXPERIMENTAL

PVA ($M_w = 89,000$ – $98,000$ g/mol and hydrolysis degree $> 99\%$) was purchased from Sigma-Aldrich and was used as received. PVA films were obtained by the dissolution of a known amount of PVA in water to obtain a 7.8 wt % solution under stirring. We prepared films by the solvent-casting method, by pouring the former solution into plastic Petri dishes and allowing the solvent to evaporate at 60°C . These films had thicknesses of about $40\ \mu\text{m}$, as measured by a Mitutoyo micrometer. A thin layer of gold was vacuum-deposited onto both film sides to

serve as electrodes. Small rectangular pieces ($4 \times 3\ \text{mm}^2$) of these films were prepared for measurements, and the contact areas were measured with a digital calibrator (Mitutoyo).

XRD measurements

Crystal structure analysis was performed with a Rigaku DMax 2100 diffractometer equipped with $\text{Co K}\alpha_1$ radiation ($\lambda = 1.7889\ \text{\AA}$) in the 2θ range from 5 to 55° at 30 , 80 , 120 , 160 , and 180°C and operating at $30\ \text{kV}$ and $16\ \text{mA}$.

The estimation of the crystalline volume fraction was based on the standard approach, which assumes that the experimental intensity curve is a linear combination of the intensities of the crystalline and amorphous phases. This means that for a material with two phases, one crystalline and one amorphous, XRD measurements can be used to determine the volume fraction of each phase. The degree of crystallinity was obtained as a relation between the integral intensities of the crystalline (I_c) and amorphous (I_a) peaks to the total integral intensity of the diffraction curves [$I_c/(I_c + I_a)$]. The values of the crystalline volume fraction were obtained with WinJADE MDI version 7.5 software.^{28,29}

Thermal and mechanical measurements

The moisture content was determined by TGA. The moisture content was evaluated by the decrease of sample weight during the heating scan. TGA curves were obtained with a Mettler Toledo apparatus (model TGA/SDTA 851e); the sample mass was about $3\ \text{mg}$, and an aluminum sample holder under an argon atmosphere with a flow rate of $75\ \text{mL}/\text{min}$ was used. The heating rate was set to $10^\circ\text{C}/\text{min}$.

DMA

DMA measurements were carried out with a TA Instruments RSAIII at a heating rate of $5^\circ\text{C}/\text{min}$ at a frequency of $0.1\ \text{Hz}$ under a dry air atmosphere in the 25 – 300°C temperature range. Two different annealing temperatures were studied, 80 and 120°C . TGA measurements for the moisture content determination for DMA measurements were performed under similar ambient and temperature conditions as in the DMA.

Dielectric measurements

Dielectric measurements in the frequency range $0.1\ \text{Hz}$ to $1\ \text{MHz}$ were carried out with a Solartron 1260 impedance gain-phase analyzer with a 1294 Impedance interface in the $100\ \text{Hz}$ to $110\ \text{MHz}$ frequency range with an Agilent Precision Impedance

Analyzer 4294A. The amplitude of the measuring signal was 100 mV. A homemade impedance vacuum cell was used in conjunction with a Watlow's Series 982 microprocessor with a ramping temperature controller for all dielectric measurements from 20 to 300°C at the two annealing temperatures, 80 and 120°C. Each sample was left at each temperature for 3 min to ensure thermal equilibrium.

RESULTS AND DISCUSSION

Moisture content

Three different moisture contents according to different sample treatments were evaluated; wet samples (without annealing treatment) and two different annealing temperatures, 80 and 120°C. Samples annealed at 80°C were obtained in the following fashion: a first scan was performed from 20 to 80°C, with holding at 80°C for 30 min and followed by cooling at 20°C; afterward, a second heating from 20 to 250°C was carried out. A similar heating-cooling-heating (H-C-H) sequence was performed in the second annealing treatment, with heating to 120°C instead of 80°C in the first scan. Before annealing, a single scan on wet PVA was performed for comparison. Thermogravimetric measurements in PVA (not shown) performed in the same H-C-H sequence indicated water losses of about 0.01, 2.78, and 4.16% for the samples annealed at 120 and 80°C and the wet sample, respectively.

The third scan, after annealing at 120°C (dry samples), revealed a water loss lower of than 0.01%, so samples annealed at 120°C did not need further heat treatment to eliminate more water. Also, annealing at 120°C induced changes in crystalline volume fraction that ultimately changed the molecular relaxations in PVA.

Dielectric relaxation analysis

The direct-current conductivity (σ_{dc}) behavior of the PVA films was analyzed by DS with the methodology that we described previously.²⁹⁻³¹ Resistance (R_{dc}) was obtained from the intersection of the semicircle and the real-part axis on the impedance plane ($Z'' = 0$), as shown in the inset of Figure 1(a); hence, σ_{dc} could be calculated by the following relationship:

$$\sigma_{dc} = d/(R_{dc} \times A)$$

where d is the thickness and A is the area of the PVA film, respectively. In the PVA complex dielectric spectra [Z'' vs Z' plot of the window inset of Fig. 1(a)] above 120°C, two different behaviors were identified: (1) a typical semicircle at high frequencies, which corresponded to the bulk material signal,

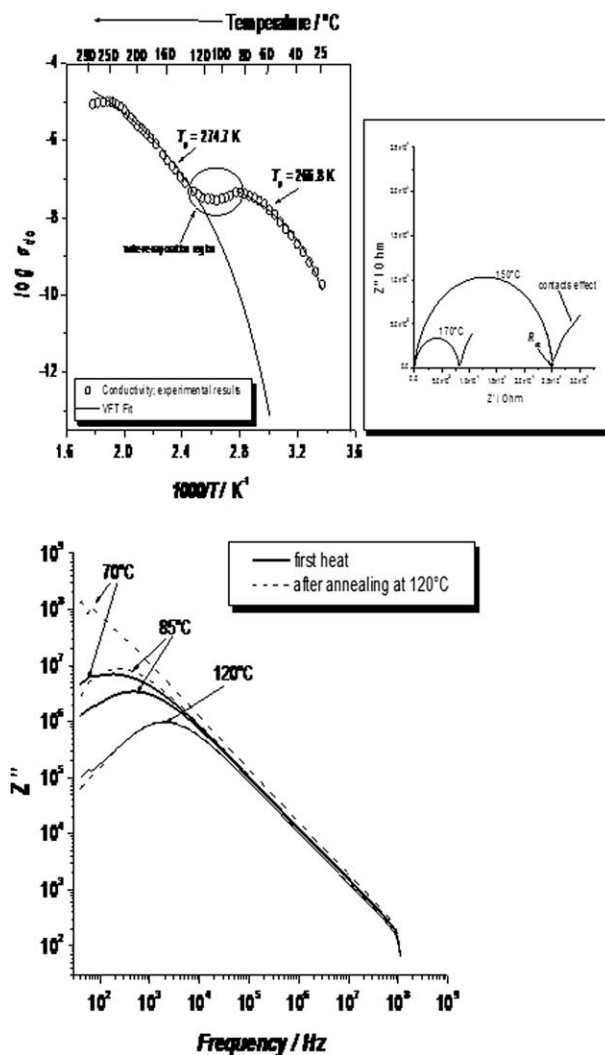


Figure 1 (a) σ_{dc} as a function of $1000/T$ (K^{-1}) for PVA (two different regions with VFT behavior were observed). Inset: R_{dc} calculated by dielectric measurements the intersection of the semicircle and $Z'' = 0$. The contact polarization effect is shown in the low-frequency side. (b) Impedance imaginary part (Z'') of the spectra versus the frequency for wet and dry PVA.

and (2) a quasi-linear response at low frequencies associated with interfacial polarization in the bulk of the films and/or surface and contact effects.²⁹ This low-frequency part of the electrical response was easily influenced by imperfect contact between the metal electrode and the sample; however, as it was previously tested elsewhere,²⁹ there was no influence of gold contact on the polymer impedance spectra (high-frequency part of the spectra corresponding to the bulk of the film), and it was discarded for further analysis.

Figure 1(a) shows the change in σ_{dc} as a function of temperature from 25 to 300°C for a wet PVA film. The conductivity increased as the temperature increased, and this dependence unveiled two well-defined regions at low and high temperatures, with

an intermediate discontinuity between 80 and 120°C associated with the moisture evaporation. Both relaxation regions disclosed a well-defined non-Arrhenius behavior usually observed in many glass formers; this behavior is described by the well-known Vogel–Fulcher–Tammann (VFT) relationship:

$$\sigma = \sigma_0 \exp(-DT/T - T_0)$$

where σ , σ_0 , and D are the direct-current conductivity, the pre-exponential factor, and a material constant, respectively, and T_0 is the so-called Vogel temperature. This model is related to the α relaxation, and it provides clear evidence of the glass-transition phenomenon; however, at this point, this behavior was not disclosed in the whole temperature range as in many amorphous polymers, such as polypeptides.³²

As it is illustrated in Figure 1(a), two different T_0 values were calculated by the fitting of the experimental data to the VFT model, described previously. The low-temperature region (<80°C) displayed a lower T_0 than the high-temperature region (>120°C); this suggested a plasticizing effect of moisture on PVA. Figure 1(a) shows two regions: one from 25 to 80°C and another one from 120 to 250°C. A transition region, in which the conductivity did not vary significantly, was observed in the 80–120°C temperature range; this transition region may have been due to moisture evaporation. This event revealed the existence of strong interactions between water and the PVA chains, and it was a good indication of the existence of strong hydrophilic groups acting as primary hydration sites: OH side groups. An overall increase in the molecular mobility with increasing water content occurred. This contribution was due to loosely bound water molecules connected to the reorientation of water molecules in water clusters around the primary hydration sites. The hydroxyl groups had strong effects on the PVA molecular dynamics because of the interactions between OH neighbors and absorbed moisture. A strong influence of the absorbed moisture on the structure and molecular mobility on the polymer materials and their blends has been reported in previous investigations,²⁴ and the produced relaxations might have played an important role in controlling the macroscopic properties.

Figure 1(b) shows the imaginary part (Z'') of the spectra as a function of frequency for wet and dry samples. The wet samples were heated to 120°C (first scan), cooled to ambient temperature, and then heated to 300°C (second scan) to produce annealed (dry) samples. During this thermal cycle, measurements were taken every 5°C, such that a complete thermal history was recorded. It is very important to emphasize that the samples treated during the first scan were the wet samples and that those treated

during the second scan were the annealed samples. For instance, the data at 70 (wet sample: first scan; annealed sample: second scan), shown in Figure 1(b), were the results from the same samples taken during the thermal cycle.

The α peak exhibited by the annealed (dry) film drastically shifted to lower frequencies for temperatures below 120°C, this implied higher τ 's and lesser mobility when the moisture content was near zero. An overall increase in the molecular mobility with increasing moisture content was shown by a shift of the dispersion to higher frequencies, which was attributed to the conductivity mechanism. This difference between the wet and dry samples was present in the spectra below 120°C. As shown by comparison of the dry and wet samples at 120°C [Fig. 1(b)], the dielectric loss was almost the same for the wet and dry states, and the water effect was absent at 120°C for moisture contents of less than 0.001% (measured by TGA, see Moisture Content section for more details). In contrast, for the annealed treatment at 80°C, an evident difference in the wet and dry spectra was observed. This confirmed that the 120°C annealing temperature was adequate for complete water removal, and moisture contents below 2.78% (the moisture content for samples annealed at 80°C) were required to preclude the water effect on the molecular dynamics of PVA. In addition, the dielectric results give no indication of the appearance of any new relaxation in the wet samples; this could have been attributed to the relaxation of the water molecules themselves; this conclusion was in agreement with similar statements in the literature.³³

On the other hand, the two different temperature regions described previously were described by Hanafy¹⁴ for pure PVA and GdCl₃-doped PVA films. Hanafy¹⁴ classified these two regions as region I, from about 30 to 60°C, and region II, from about 84 to 135°C, to propose two Arrhenius-type relaxations for pure PVA films. However, if we compare the data of Hanafy to our study in the same temperature range, as plotted in Figure 2(a), one may argue the validity of the two linear relationships (Arrhenius type) of the conductivity with reciprocal temperature. However, when the data are taken up to 300°C [see Fig. 1(a)], a non-Arrhenius-type relationship was evidenced in both the low- (25–80°C) and high- (120–250°C) temperature regions. This subtlety was previously addressed by our group in polysaccharides and polysaccharides nanocomposites to resolve a non-Arrhenius-type versus an Arrhenius-type relaxation controversy.^{29–31}

In the previous context, Bhargav et al.¹ reported a single Arrhenius behavior for the dependences of the conductivity and τ in the 30–100°C temperature range for pure PVA and PVA complexed with NaI

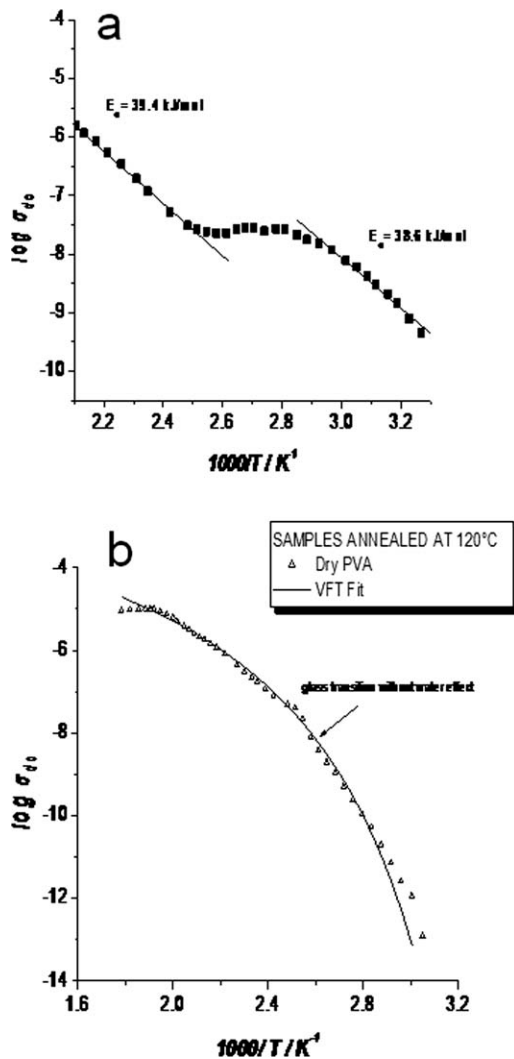


Figure 2 (a) σ_{dc} as a function of $1000/T$ (K^{-1}) in the temperature range commonly evaluated by other authors.¹⁴ Two Arrhenius-type behaviors seemed to be displayed. (b) $\log \sigma_{dc}$ versus $1000/T$ for dry PVA. VFT was extended in the whole temperature range after annealing at $120^\circ C$.

salt, but their activation energy (E_a) was almost two times lower than that of Hanafy.¹⁴ Bhargav et al.¹ attributed this relaxation process to β relaxation due to the orientation of the side groups. In the 27 – $127^\circ C$ temperature range, Migahed et al.¹³ calculated the activation energies of pure PVA and lead salt–PVA composites using the Arrhenius behavior described by the τ versus reciprocal temperature dependence. Similarly, Singh and Gupta¹⁵ reported similar activation energies for PVA– H_3PO_4 and PVA– H_2SO_4 complex electrolytes. Dielectric secondary relaxations in hydrated and dried PVA were reported by De la Rosa et al.²¹ in the -133 to $127^\circ C$ temperature range. They observed only one broad secondary relaxation process, assigned as a β relaxation, with 74 and 59 kJ/mol activation energies for hydrated and dried PVA, respectively, and ascribed it to the rotation of

the hydroxyl groups. $\log \Phi$ versus $1/T$ (where T is the temperature) plots of PVA/montmorillonite composites, also with Arrhenius-type dependences, were shown by Yang et al.²⁰ with activation energies of about 10.62 kJ/mol. There exist other reports following the same Arrhenius-trend below $135^\circ C$ in different PVA-based materials^{25–27} that claim that at this point, the β relaxation manifests because of side-group motion.

Regarding the VFT behavior related to the glass transition; Agrawal et al.¹² observed this nonlinear behavior on the conductivity plot from 14 to $100^\circ C$ in pure PVA and PVA with ammonium salt films, but no further discussion was provided on the nature of the relaxations in these materials. Another report suggesting VFT behavior were provided by Rajendran et al.¹⁸ in the 29 – $100^\circ C$ temperature range for PVA/poly(methyl methacrylate) blends and for Linares et al.⁵ in the 30 – $110^\circ C$ temperature range in PVDF/PVA blends; this suggested a $T_g = 314.9$ K $\approx 41.72^\circ C$ for pure PVA defined at $\tau = 100$ s.³⁴

On the basis of the data reported in Figure 1(a) in the 30 – $80^\circ C$ range, we propose that the wet PVA film exhibited three structural changes:

1. A depressed T_g of PVA of about $44^\circ C$, which was described by a VFT model and not an Arrhenius-type model.
2. A transition region in the 80 – $120^\circ C$ range. In this transition region, the conductivity decreased slightly because of water evaporation.
3. Melting point onset at 250 – $300^\circ C$.

A VFT fitting in the high-temperature region (120 – $250^\circ C$) allows one to perform an extrapolation to lower temperatures. This extrapolation suggests a continuation of the primary relaxation at high temperatures that extends to lower temperatures, about $60^\circ C$ [see model extrapolation in Fig. 1(a)]. Under special sample conditions, the low-temperature region will vanish and, thus, reveal a single VFT-type relaxation. We performed dielectric measurements on samples of controlled moisture contents on the basis of these observations. We studied PVA films annealed at $120^\circ C$ (moisture content $< 0.01\%$ as calculated by TGA not shown) and wet samples with moisture contents of less than 4.16% . The results are shown in Figure 2(b).

Figure 2(b) shows that the dry (annealed) PVA films only exhibited one VFT-type relaxation in the whole temperature range of our study and that the low-temperature region vanished (in the wet samples). These results strongly suggest that the low-temperature region in the wet samples was related to the depressed T_g . The high-temperature region (after moisture evaporation) was the VFT-type trace of the dry PVA films. This is shown

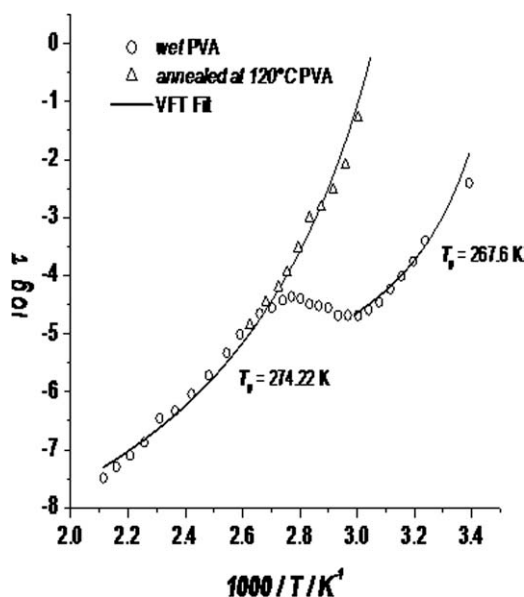


Figure 3 τ behaviors for the wet and annealed (dry) PVA films. A transition region in the range 80–120°C similarly observed in the conductivity behavior [see Fig. 1(a) and text for more details].

exactly in Figure 3, where the wet and dry (annealed) PVA films are compared. Calculations of the VFT model showed that T_0 for dry PVA obtained from the conductivity plot was 274.7 K. It has been demonstrated that for most polymers, the relationship between T_g and T_0 is $T_g = T_0 + 50$ K.^{35–37} On this basis, a T_g of 324.7 K = 51.5°C can now be proposed from the dielectric measurements of the dry PVA films. It is important to note that the narrow temperature range previously analyzed by other authors could lead to different interpretations and that the real PVA molecular dynamics explanation could be inaccurate.

It has recently been recognized that contact and interfacial polarizations need to be accounted for when one analyzes dielectric spectra. Indeed, it is well known that σ_{dc} strongly affects the loss factor (ϵ'') in the low-frequency range, and a correction must be applied to unmask the polymer dielectric effects.²⁹ The σ_{dc} and contact polarization effect could mask the real dielectric relaxation processes in the low-frequency range; therefore, to analyze the dielectric processes in detail, the complex permittivity (ϵ^*) is converted to the complex dielectric modulus (M^*) by the following equation:

$$M^* = 1/\epsilon^* = M' + iM'' = [\epsilon'/(\epsilon'^2 + \epsilon''^2) + i\epsilon''/(\epsilon'^2 + \epsilon''^2)]$$

where M' and M'' are the real and imaginary parts of the electric modulus, respectively, and ϵ' and ϵ'' are the real and imaginary parts of the permittivity, respectively. The dielectric modulus

is commonly used to analyze dielectric experimental data because the interfacial polarization, electrode contribution, and direct-current conductivity effects do not affect the M'' peak. M'' is temperature dependent.³⁸

The τ was obtained for each temperature from the maximum of the imaginary part of the dielectric modulus ($\tau = 1/2B f_{max}$, where f_{max} is the frequency at the maximum of the M'' peak). The M'' peak is shown in Figure 4(a). As shown in Figure 4(a), the wet films displayed a trend akin to the conductivity as the temperature increased; two VFT behaviors in the high- and low-temperature ranges were separated by a moisture evaporation effect in the

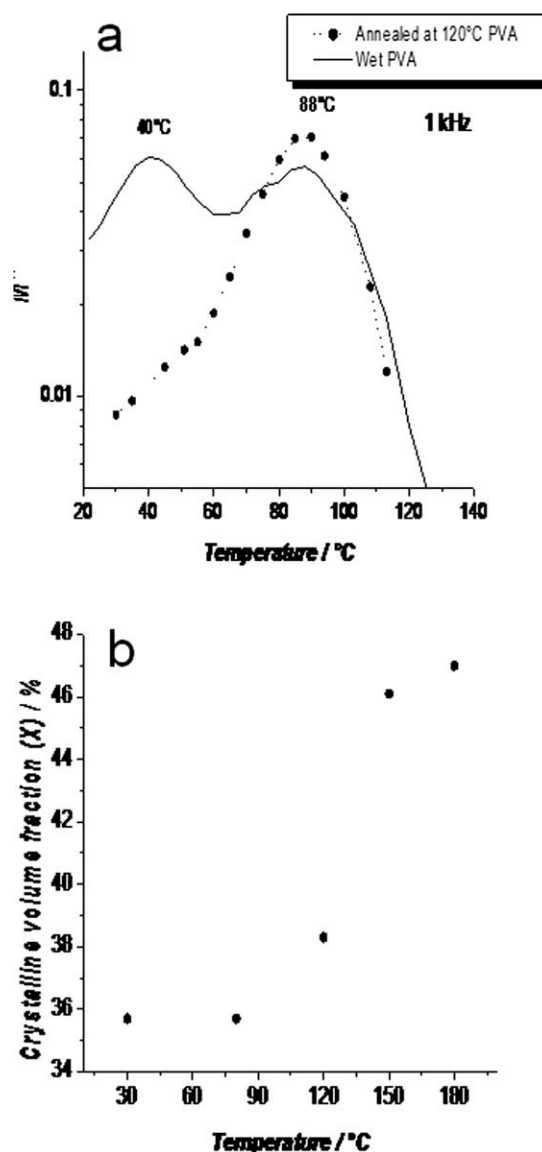


Figure 4 (a) Variation of the imaginary component of the modulus (M'') with temperature in PVA. The low-temperature relaxation vanished after annealing. (b) XRD crystalline volume fraction at different temperatures.

80–120°C temperature range. T_0 was calculated from the VFT model for τ as follows:

$$\tau = \tau_0 \exp(DT_0/T - T_0)$$

where τ_0 and D are the pre-exponential factor and a material constant, respectively. From the τ data (Fig. 3), the results were in agreement with those obtained by the conductivity plot [Fig. 1(a)]. The observed T_g is commonly considered as the temperature at which the characteristic τ of the material equals about 100 s.^{34,38} With this assumption and the calculated VFT parameters for dry PVA, we determine that T_g ($\tau = 100$ s) = 52.5°C; this was in excellent agreement with the $T_g = T_0 + 50$ K rule.

More information about the moisture effect was provided by means of M^* , specifically by the imaginary component (M''), a common parameter used to investigate the relaxation processes in polymers. The M'' versus temperature plot for the wet and dry PVA samples is shown in Figure 4(a). In the wet samples (solid line), two relaxations peaks at 40 and 88°C for 1 kHz were found. As the frequency increased, both peaks shifted toward higher temperatures (not shown). These two relaxation peaks were previously reported by other authors from M'' , ϵ'' , and $\tan \delta$ plots for pure PVA and PVA blends and composites.^{1,5,13–15} These relaxations were assigned as the β relaxation ascribed to side-group dipole ($T_\beta = 40^\circ\text{C}$) orientation and the glass transition of PVA (ca. $T_g = 85^\circ\text{C}$), respectively.^{1,5,13–15} Nonetheless, our results show that for dry samples, the lower temperature relaxation peak (40°C) vanished after the PVA films were annealed at 120°C; the α -relaxation peak remained at the same temperature for each frequency. This fact led us to conclude that the low-temperature relaxation in wet PVA could be traced to a moisture effect, and it did not correspond to a local-mode β relaxation. In our study, for dry samples, T_g was about 88°C.

PVA and moisture interaction corresponded to the formation of hydrogen bonds between PVA hydroxyl groups and water, and hydrogen bonds were the dominant interaction responsible for the structure and its molecular dynamics. It is possible that the interaction between the OH groups and moisture was capable of destroying the interchain and intrachain bonding in PVA affecting its crystalline regions; therefore, water acted as a plasticizer by increasing the free volume in the amorphous phase.²²

Figure 4(b) shows the XRD change in the crystalline volume fraction of the PVA films at different temperatures. The PVA crystallinity began to increase above 80°C, so the observed variation of M'' with temperature in the wet films indicated that the origin of the first peak (at 40°C) was not a reorientational relaxation of dipoles but the mobility of

weakly bonded water molecules causing an inhomogeneous distribution of dipoles and changes on the molecular level.²² The PVA crystallinity above 120°C, in the absence of moisture, increased from about 36% to about 47%; this suggested that the molecular relaxations were greatly affected.

Heating to 120°C gave rise to a loss of moisture (moisture content < 0.01%); it contributed to the increase of the crystallinity of PVA by the formation of intrachain and interchain hydrogen bonding, which affected the crystalline and amorphous phases. This gave rise to an increase in the PVA crystallinity and changes in the relaxation behavior.

DMA

The $\tan \delta$ damping factor of pure PVA is shown in Figure 5. The two different annealing temperatures, 80°C [2.78% moisture content, Fig. 5(a)] and 120°C [0.01% moisture content, Fig. 5(b)], shown previously by DS analysis, were investigated by DMA. In both Figure 5(a) and 5(b), there is one clear $\tan \delta$ peak below 100°C in both H–C–H cycles; it was assigned as the α relaxation of PVA. A second peak of about 140°C [Fig. 5(b)] was ascribed to the so-called β_c relaxation caused by changes in the crystalline volume fraction, as pointed out by Nishio and Manley.²³ A third transition above 200°C represented the PVA melting point.

The relaxation below 100°C was related to the low-temperature DS relaxation discussed previously; this was associated with T_g of PVA and the effect of water. From Figure 5, one can estimate T_g from DMA. For wet samples, $T_g = 62.7^\circ\text{C}$. For samples annealed at 80°C, $T_g = 76.6^\circ\text{C}$, and for dry samples annealed at 120°C, $T_g = 82.4^\circ\text{C}$; this value was close to the commonly accepted T_g value. T_g shifted to higher temperatures because of a decrease in moisture content originated by the annealing treatment; this was in agreement with other reports.^{15,17}

As in the DS measurements, the 120°C annealing temperature was more suitable for water elimination than the one given for the 80°C H–C–H sequence, in which the effect of water was still evident. When water was present, it gave rise to less intense and broader peaks values with a little superposed shoulder below 50°C; consequently, a lower T_g was exhibited [see Fig. 5(a)]. For this reason, for sample treatment at 80°C, a small amount of water was eliminated; this, therefore, influenced the value of the glass transition. That is, temperatures above 120°C were needed to eliminate the water effect on T_g .

Nishio and Manley,²³ using DMA, suggested two peaks located at about 80 and 35°C, and they were related to α relaxation (glass transition) and to the β_a relaxation associated with a local relaxation mode of PVA, respectively. On the basis of the DS analysis

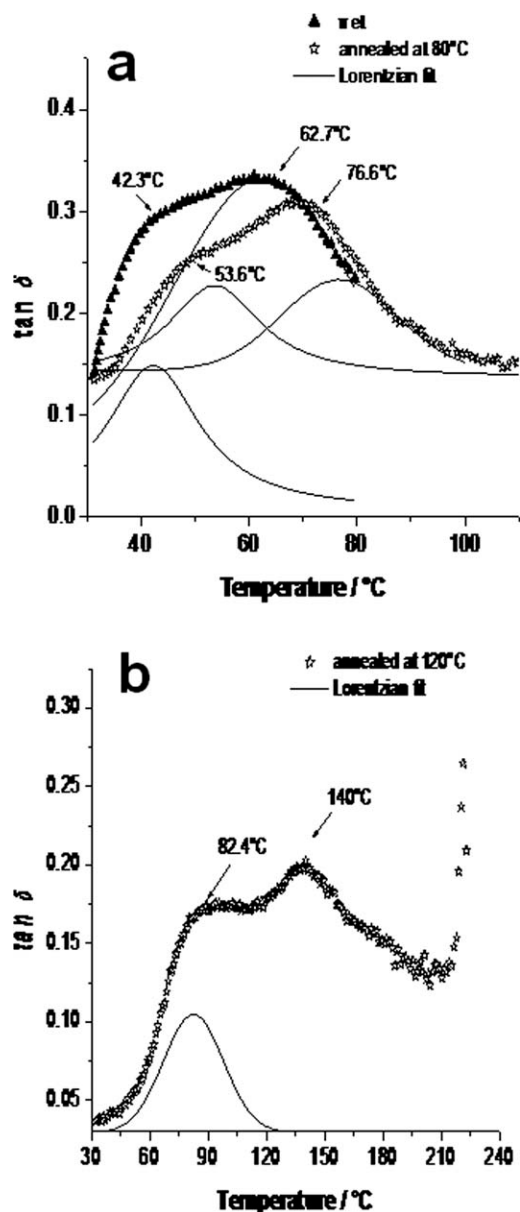


Figure 5 $\tan \delta$ versus the temperature for PVA annealing at (a) 80 and (b) 120°C. The $\tan \delta$ peaks for PVA annealing at 80°C were not well defined; a shoulder was observed below 50°C. The moisture plasticized PVA, shifting T_g to a higher temperature as the moisture content decreased.

mentioned previously, β_a relaxation seemed to be traceable to the water content effect. As explained previously, as shown in Figure 5(a), there was a shoulder below 50°C that precluded a clear definition of the peak associated with the α relaxation, and it was related to the β_a relaxation. This shoulder vanished when the samples were annealed at 120°C. As a result, the so-called β_a relaxation vanished. In this study, $T_g = 82.4^\circ\text{C}$ in dry PVA obtained by DMA; this value was higher compared to the $T_g = 51.5^\circ\text{C}$ value obtained by DS. This difference arose because DS is sensitive to changes in the orientation

of dipole moments under an applied alternating-current field, whereas DMA is sensitive to the anisotropy of the local volume change involved in the motion of molecular groups.²¹

As shown by XRD analysis in Figure 4(b), the crystalline volume fraction increased from about 36% to about 47% when the temperature increased from 30 to 180°C. Strictly speaking, this difference in the crystalline volume fraction indicated that a different molecular rearrangement took place. Figure 5(b) shows a secondary peak at about 140°C, which could be traced to a crystallization effect. This observation was in agreement with that of Nishio and Manley.²³ This relaxation was tagged as β_c , as explained previously.

In summary, it is very important to understand the nature of the different relaxation processes found in PVA because it is a commonly used polymer in blends and composite materials in many technologically important applications. An inaccurate interpretation of the dielectric and dynamic mechanical results can lead to a misunderstanding of the nature of the PVA molecular dynamics relevant in the miscibility of polymer blends, as in the mechanical and dissolution properties.

CONCLUSIONS

The molecular dynamics of PVA were studied by DS and DMA. Improper water elimination analysis has led to the misinterpretation of the thermal relaxations in PVA, such that a depressed T_g for wet PVA films (ca. 40°C) has been assigned as a secondary β relaxation in a number of previous studies in the literature. In wet PVA samples, two different VFT behaviors separated by the moisture evaporation region (from 80 to 120°C) were observed in the low- (from 20 to 80°C) and high- (>120°C) temperature ranges. Previously, these two regions were erroneously assigned to two Arrhenius-type relaxations. However, once moisture was properly eliminated, a single α , non-Arrhenius, VFT-type relaxation was clearly revealed. When the samples were annealed above 120°C, moisture was minimal, and a secondary relaxation was revealed. This β_c relaxation was related to a change in the crystalline volume fraction, as previously reported.

The authors thank J. A. Muñoz-Salas from Cinvestav-QRO for assistance with the electrical measurements and Martin A. Hernández-Landaverde.

References

- Bhargav, P. B.; Sarada, B. A.; Sharma, A. K.; Rao, V. V. R. N. *J Macromol Sci Pure Appl Chem* 2010, 46, 131.
- Pawde, S. S.; Deshmukh, K. *J Appl Polym Sci* 2008, 109, 3431.

3. Raju, CH. L.; Rao, J. L.; Reddy, B. C. V.; Brahmam, K. V. *Bull Mater Sci* 2007, 30, 215.
4. Lagashetty, A.; Havanoor, V.; Basavaraja, S.; Venkataraman, A. *Bull Mater Sci* 2005, 28, 477.
5. Linares, A.; Nogales, A.; Rueda, D. R.; Ezquerro, T. A. *J Polym Sci Part B: Polym Phys* 2007, 45, 1653.
6. Lee, Y. M.; Kim, S. S. *Korea Polym J* 1996, 4, 178.
7. Gautam, A.; Ram, S. *Mater Chem Phys* 2010, 119, 266.
8. Miaudet, P.; Derre, A.; Maugey, M.; Zakri, C.; Piccione, P. M.; Inoubli, R.; Paulin, P. *Science* 2007, 318, 1294.
9. Cendoya, I.; López, D.; Alegría, A.; Mijangos, C. *J Polym Sci B: Polym Phys* 2001, 39, 1968.
10. Brostow, W.; Chiu, R. I.; Kalogeras, M.; Vassilikou-Dova, A. *Mater Lett* 2008, 62, 3152.
11. Jadhav, N. R.; Gaikwad, V. L.; Nair, K. J.; Kadam, H. M. *Asian J Pharm* 2009, 3, 82.
12. Agrawal, S. L.; Awadhia, A. *Bull Mater Sci* 2004, 27, 523.
13. Migahed, M. D.; Bakr, N. A.; Abdel-Hamid, M. I.; El-Hanafy, O.; El-Nimr, M. *J Appl Polym Sci* 1995, 59, 655.
14. Hanafy, T. A. *J Appl Polym Sci* 2008, 108, 2540.
15. Singh, K. P.; Gupta, P. N. *Eur Polym J* 1998, 7, 1023.
16. Sarti, B.; Scandola, M. *Biomaterials* 1995, 16, 785.
17. Park, J. S.; Park, J. W.; Ruckenstein, E. *J Appl Polym Sci* 2001, 80, 1825.
18. Rajendran, S.; Sivakumar, M.; Subadevi, R. *Mater Lett* 2004, 58, 641.
19. Hema, M.; Selvasekerapandian, S.; Hirankumar, G. *Ionics* 2007, 13, 483.
20. Yang, C. C.; Lee, Y. J.; Yang, J. M. *J Powder Sources* 2009, 188, 30.
21. De la Rosa, A.; Heux, L.; Cavaille, J. Y. *Polymer* 2001, 42, 5371.
22. Hernández, M. C.; Suárez, N.; Martínez, L. A.; Feijoo, J. L.; Mónaco, S. L.; Salazar, N. *Phys Rev E* 2008, 77, 051801.
23. Nishio, Y.; Manley, R. S. J. *Macromolecules* 1988, 21, 1270.
24. Pissis, P. *Electromagnetic Aquametry: Water in Polymers and Biopolymers by Dielectric Techniques*; Springer: Berlin, 2005.
25. Ogura, K.; Tonosaki, T.; Shiigi, H. *J Electrochem Soc* 2001, 148, H21.
26. Hema, M.; Selvasekarapandian, S.; Arunkumar, D.; Sakunthala, A.; Nithya, A. *J Non-Cryst Solids* 2009, 355, 84.
27. Harun, M. H.; Saion, E.; Kassim, A.; Hussain, M. Y.; Mustafa, I. S.; Omer, M. A. A. *Malaysian Polym J* 2008, 3, 27.
28. Caban, R.; Nitkiewicz, Z. J. *Achiev Mater Manuf Eng* 2007, 23, 55.
29. Gonzalez-Campos, J. B.; Prokhorov, E.; Luna-Barcenas, G.; Mendoza-Galvan, A.; Sanchez, I. C.; Nuno Donlucas, S. M.; Garcia-Gaitan, B.; Kovalenko, Y. *J Polym Sci Part B: Polym Phys* 2009, 47, 932.
30. Gonzalez-Campos, J. B.; Prokhorov, E.; Luna-Barcenas, G.; Fonseca-Garcia, A.; Sanchez, I. C. *J Polym Sci Part B: Polym Phys* 2009, 47, 2259.
31. Gonzalez-Campos, J. B.; Prokhorov, E.; Luna-Barcenas, G.; Sanchez, I. C.; Lara-Romero, J.; Mendoza-Duarte, M. E.; Villasenor, F.; Guevara-Olvera, L. *J Polym Sci Part B: Polym Phys* 2010, 48, 739.
32. Lee, A. L.; Wand, A. J. *Nature* 2001, 411, 501.
33. Schartel, B.; Wendling, J.; Wendorff, J. H. *Macromolecules* 1996, 29, 1521.
34. Saiter, J. M.; Grenet, J.; Dargent, E.; Saiter, A.; Delbreilh, L. *Macromol Symp* 2007, 258, 152.
35. Yang, J. M.; Su, W. Y.; Leu, T. L.; Yang, M. C. *J Membr Sci* 2004, 236, 39.
36. Lee, A. L.; Wand, A. J. *Nature* 2001, 411, 501.
37. Raju, G. G. *Dielectrics in Electrical Fields*; Marcel Dekker: New York, 2003.
38. Köhler, M.; Lunkenheimer, P.; Loidl, A. *Eur Phys J E* 2008, 27, 115.